ELSEVIER

Journal of Alloys and Compounds 321 (2001) 307–313

Journal of ALLOYS AND COMPOUNDS

www.elsevier.com/locate/jallcom

The development of hydrogen storage alloys and the progress of nickel hydride batteries

Kuochih Hong

Hong Enterprises, Troy, MI 48098, USA

Received 5 September 2000; accepted 5 December 2000

Abstract

In this paper, we discuss the fundamentals of a hydrogen storage alloy used as the active material in a hydride electrode and the operation principle of a rechargeable nickel hydride (NiMH) battery. We also describe briefly a semi-empirical electrochemical–thermodynamic approach to develop/screen a hydrogen storage alloy for electrochemical application. Finally, the current state of the NiMH batteries including commercial manufacture process, cell performance and applications is given.

Keywords: Hydrogen storage; Hydride batteries

1. Introduction

Studies in metal–hydrogen grew rapidly in the 1970s due to the hydrogen storage programs for the alternative energy research looking for clean energy system. As a result, many metal–hydrogen systems and hydride alloys were studied and/or developed [1–5]. One of the fruits of these studies was the development of metal hydride technology, more specifically the commercial rechargeable nickel hydride batteries in the 1980s. The mass commercial nickel hydride (NiMH) batteries began in the early 1990s. In 1999, sales of NiMH cells was estimated to be about 900 million cells. Compared to the NiCd battery, a NiMH cell has several advantages such as about twice the capacity, no memory effect, and no environmental pollution problem. The NiMH battery is in a very rapid speed to replace the nickel cadmium (NiCd) battery.

As one of the early investigators in commercialization of NiMH batteries, especially in the development of high capacity and long life hydrogen storage electrode materials [6,7], in this paper we will give a review and the prospect of the hydrogen storage electrode alloys and NiMH batteries.

2. The fundamental concept of hydride electrode and NiMH battery

2.1. Hydride electrode

The interaction of hydrogen and metal M is represented as:

$$M\,(s) + x/2\ H_2(g) \rightleftarrows MH_x\,(s) \tag{1}$$

where MH_x is the hydride of metal M. The amount of hydrogen stored in M, $x=[H/M]$, is controlled by the hydrogen equilibrium pressure P_{H_2} as shown in Eqs. (2a)–(2c), assuming that the activities of M, [M], can be considered as constant.

$$x = K_{eq}\, P_{H_2}^{x/2} \tag{2a}$$

$$\ln K_{eq} = \ln x - x/2 \ln P_{H_2} \tag{2b}$$

$$G_H = -xRT/2 \ln P_{H_2} + RT \ln x \tag{2c}$$

where K_{eq} and G_H are the hydrogen equilibrium constant and partial molar free energy, respectively. When $x=1$, we have the Sievert equation:

$$x = K_{eq}\, P_{H_2}^{1/2}$$

Some alloys can be charged and discharged electrochemically. In this case, the alloy itself is an electrochemical catalyst as well as a hydride former. Eq. (3) shows the electrochemical charging (forward) and discharge (reverse) reactions.

$$M + xH_2O + xe^- \rightleftarrows MH_x + x\,OH^- \qquad E^\circ \tag{3}$$

This reaction is competing with hydrogen evolution shown in Eq. (4).

0925-8388/01/$ – see front matter
PII: S0925-8388(01)00957-4

$$xH_2O + x\,e^- \rightleftarrows x/2\,H_2 + x\,OH^- \qquad E_2 \tag{4}$$

The relationship between equilibrium pressure (Eq. (2c)) and the half-cell potential of a hydride electrode shown in Eq. (3) is readily obtained as given in Eq. (5).

$$E^\circ = E_2 + RT/xF \ln x - RT/2F \ln P_{H_2} \tag{5}$$

At 25°C, E_2 (vs. S.H.E) = −0.828 V and E_2 (vs. Hg/HgO) = −0.925 V, so we have:

$$E^o\,(\text{vs. S.H.E}) = -0.828 - 0.0296 \log P_{H_2} + 0.0592/x \log x \tag{6a}$$

$$E^\circ\,(\text{vs. Hg/HgO}) = -0.925 - 0.0296 \log P_{H_2} + 0.0592/x \log x \tag{6b}$$

From Eqs. (5)–(6b), one can predict the half-cell potential (vs. S.H.E), E°, of a hydride electrode from P–C (pressure–composition) isotherms, and vice versa.

2.2. Ni–MH_x battery

The combination of a hydride electrode with a nickel positive electrode used in a NiCd cell can form a NiMH cell. The electrochemical reaction of a NiMH cell can be represented by the following half-cell reactions:

2.2.1. Normal charge–discharge reactions (forward reaction is charging, the reverse reaction is discharging)

Nickel positive electrode

$$x\text{Ni(OH)}_2 + x\text{OH}^- \rightleftarrows \text{NiOOH} + x\,H_2O + x\,e^- \tag{7}$$

Hydride negative electrode

$$M + x\,H_2O + x\,e^- \rightleftarrows MH_x + OH^- \tag{8}$$

Overall reaction:

$$x\,\text{Ni(OH)}_2 + M \rightleftarrows x\,\text{NiOOH} + MH_x \tag{9}$$

Eq. (9) indicates that ideally there is no net change in water and OH^- ions in the overall reaction of a NiMH cell.

2.2.2. Overcharge

In the actual cell construction, especially a sealed cell, the capacity of the hydride negative electrode is higher than that of the nickel positive electrode. This is the positive-limited cell to prevent the internal pressure build-up during overcharge. During overcharge, oxygen evolution will occur in the positive electrode, but the hydride electrode will be charged further initially. The oxygen generated will diffuse to the hydride negative electrode to combine the hydrogen to form water. This is the so-called oxygen recombination in the battery. Therefore, the internal pressure build-up will be eliminated or reduced substantially. In practice, the oxygen generated would react with the alloy to form oxides at least partially. Also, hydrogen evolution often occurs in the high current charging. All the main reactions during overcharge are given in Eqs. (10)–(12c).

Nickel electrode:

$$2y\text{OH}^- \rightleftarrows y\,H_2O + y/2\,O_2 + 2y\,e^- \tag{10}$$

Hydride electrode:

$$MH_x + 2y\,H_2O + 2y\,e^- \rightleftarrows MH_{x+2y} + 2y\,OH^- \tag{11}$$

$$y/2\,O_2 + MH_{x+2y} \rightleftarrows MH_x + y\,H_2O \tag{12a}$$

Actual (non-ideal) case

$$z/2\,O_2 + MH_x \rightleftarrows MH_{x-2z}\,O_z + z\,H_2 \tag{12b}$$

$$q\,H_2O + q\,e^- \rightleftarrows q\,OH^- + q/2\,H_2 \tag{12c}$$

2.2.3. Over-discharge

For a positive-limited and negative precharged NiMH cell, the hydride electrode has more capacity and is partially precharged. In this cell, the nickel electrode will discharge completely first. Therefore, hydrogen evolution will occur at the nickel electrode during over-discharge, but the hydride negative electrode will continue discharge and no oxygen evolution occurs initially (at low current). The hydrogen generated at the nickel electrode will diffuse to the hydride electrode and be absorbed by the hydrogen storage alloy in the electrode. Thus, the hydride electrode will not be oxidized and no internal pressure is built-up in a sealed cell. These reactions are given in the following equations:

At nickel electrode

$$p\,H_2O + p\,e^- \rightleftarrows p\,OH^- + p/2H_2 \tag{13}$$

At hydride electrode

$$MH_p + p\,OH^- \rightleftarrows M + p\,H_2O + p\,e^- \tag{14}$$

$$M + p/2H_2 \rightleftarrows MH_p \tag{15}$$

In a prolonged and/or in a high current over-discharge process, the hydrogen recombination rate at the hydride electrode generally is not fast enough to keep recharging the hydride electrode. Therefore, the electrode will eventually discharge completely and oxygen evolution will occur. Consequently the internal pressure of the cell will build up

and the hydride electrode may be partially oxidized and damaged.

3. The development of commercial hydrogen storage electrode alloys

3.1. Criteria of a good hydride electrode alloy

Not every hydrogen storage alloy can be charged and discharged electrochemically. As the active material of a hydrogen storage electrode, a hydrogen storage alloy has several roles: an electrochemical catalyst for hydrogen generation and a hydrogen storage reservoir during charge and, a hydrogen source and an electrochemical catalyst for hydrogen oxidation during discharge. Therefore, a good hydrogen storage (hydride) electrode material must have the following properties:

1. High reversible hydrogen storage capacity, >1 wt.%.
2. Good electrochemical catalyst for hydrogen atom generation and oxidation.
3. Excellent corrosion resistance in alkaline electrolyte.
4. Suitable hydrogen equilibrium pressure, not higher than 5 atm at 25°C.
5. Good charge/absorption and discharge/desorption kinetics and efficiency.
6. Long cycle life.
7. Small hysterisis in charge/discharge (absorption/desorption) isotherms.
8. Low cost

3.2. Stages of the hydrogen storage electrode alloy development

1. In the 1970s, the concept of a hydrogen storage alloy for the electrochemical application was initiated [8–15]. However, researchers were using trial–error method testing the known hydrogen storage materials such as TiNi, TiFe, $LaNi_5$. As a result, there was not much progress in developing a reliable and useful alloy for the commercial application.
2. In the early 1980s, Hong [6,7] first studied Ti/Zr-based AB_2 type Ti/Zr–V–Ni–M systems and Willems [16,17] reported rare earth-based AB_5 type Ln–Ni–Co–Mn–Al alloys. Both obtained long life hydrogen storage electrode alloys, but the Ti/Zr system has a higher capacity. These new materials opened the window for the commercialization of rechargeable nickel hydride batteries.
3. In the late 1980s and early 1990s, Hong [18,19] and Gamo et al. [20], away from the stoichiometric restriction of AB_2 and AB_5 types, independently studied AB_x type alloys. As a result, more new alloys having improved performance including more capacity and/or long cycle life were developed.

3.3. A semi-empirical method to develop a hydrogen storage electrode alloy

In the 1970s and early 1980s, the development of a hydrogen storage electrode material was done by trial and error method. It was time-consuming and wasted a lot of man-power and expenses. To solve this problem, Hong [18,19,21–23,33], based on the thermodynamic and electrochemical studies, presented a semi-empirical method to develop good hydrogen storage electrode alloys.

According to Hong, a potential candidate alloy, $A_aB_bC_c\ldots$ for rechargeable hydrogen storage electrode has to satisfy three basic conditions: (a) $A_aB_bC_c\ldots$ contains at least 5–85 at.% of Ni, preferably 15–65 at.%, (b) contains at least 10–80 at.% of hydride formers selected from Ti, Zr, V, rare earth metals and Nb, preferably 15–65 at.%, and (c) the calculated heat of hydride formation H_h is between -2.5 and -10.50 kcal mole^{-1} H. When the elements A, B, C, ... are chosen, a set of atomic ratio, a, b, c, ... can be obtained by the following equation:

$$H_h = \frac{[aH_h(A) + bH_h(B) + cH_h(C) + \ldots]}{(a + b + c + \ldots)} + K \qquad (16)$$

where $H_h(A)$, $H_h(B)$, $H_h(C)\ldots$ are the heat of hydride formation of the elements A, B, C, ... respectively, in the unit of kcal mole^{-1} H (or kcal mole^{-1} H_2); K is a constant depending on the heat of formation, H^f, of the alloy, $A_aB_bC_c\ldots$ and the heat of mixing, H_h^m, of the hydrides AH, BH, CH, ...

$$K = -H^f/(a + b + c + \ldots) + H_h^m \qquad (17)$$

If H^f and H_h^m are set to be -7.85 kcal mole^{-1} alloy and -2.8 kcal mole^{-1}, respectively [18,19], the values of K are 0.5, -0.2 and -1.5 kcal mole^{-1} H for $a + b + c\ldots$ equal to 2, 3 and 6, respectively. For $a + b + c + \ldots$ not equal to 2, 3 and 6, it can be normalized to 3 for Ti/Zr-based alloy and 6 for rare earth-based alloy before calculation.

The amount of nickel content controls the kinetics of electrochemical reactions, while the heat of hydride formation controls the hydrogen storage capacity and the hydrogen absorption/desorption diffusion rate. The heats of hydride formation of metals, in kcal mole^{-1} H_2, are given as:

$H_h(Mg) = -17.9$, $H_h(Ti) = -15.0$,

$H_h(V) = -7.0$, $H_h(Cr) = -1.81$, $H_h(Mn) = -2.0$,

$H_h(Fc) = 4.0$, $H_h(Co) = 3.5$, $H_h(Ni) = 1.8$,

$H_h(Al) = -1.38$, $H_h(Y) = -27$,

$H_h(Zr) = -19.5$, $H_h(Nb) = -9.0$,

$H_h(Pd) = -4.0$, $H_h(Mo) = -1.0$, $H_h(Ca) = -21.0$,

H_h(Si) = −1.0, H_h(C) = −1.0, H_h(Cu) = 2.0,
H_h(Ta) = −10.0, H_h(Sn) = 2.05,

H_h(rare earth metals) = −27.0, H_h(Li) = −21.0,
H_h(Na) = −13.4, H_h(K) = −13.7,

H_h(Rb) = −12.5, H_h(B) = 2.83, H_h(Sb) = 5.5,
H_h(Y) = −20.2, H_h(Sc) = −28.9,

H_h(Zn) = −1.2, H_h(Ag) = 1.0, H_h(S) = −1.0,
H_h(N) = −0.5, H_h(W) = −0.50, and H_h(P) = −0.30.

From Eq. (16) and the boundary conditions of the heat of hydride formation mentioned above, and the known heats of hydride formation of the given elements A, B, C, ..., a set of *a*, *b*, *c*, ... and therefore, the potential alloys can be obtained by computer calculation and then made by vacuum melting. This approach can be applied to both for the transition metal-based alloys and rare earth-based alloys. However, it should be noted that: (a) for the Ti/Zr-based alloy, the heat of hydride formation is preferably in the range between −4.5 and −8.0 kcal mole^{-1} H, (b) for the rare earth-based alloys, the heat of hydride formation is preferably between −3.50 and −5.40 kcal mole^{-1} H, and (c) for the high rate application, the nickel content of the alloy is not less than 35 at.%, preferably greater than 43 at.% for the Ti/Zr-based alloy and is not less than 50 at.% for the rare earth-based alloy.

This semi-empirical approach has been found very useful in developing new hydride electrode alloys [18,19,21–29,33]. We strongly believe that the electrochemical performance and the crystal structure of an alloy are both the results of the microscopic electronic configuration and therefore, are determined by the electrochemical–thermodynamic properties. Consequently this thermodynamic and electrochemical approach is totally free of the crystal structure restriction. The alloys developed can be multiphases, polycrystalline, microcrystalline and/or amorphous. Table 1 lists some useful hydrogen storage electrode alloys including both Ti/Zr-based and Mm-based alloys (Mm is the mischmetal, a mixture of rare earth metals). Table 2 shows the comparison of the electrochemical performance between AB_x type Ti/Zr-based and rare earth based alloys. In general, a Ti/Zr-based alloy having the calculated heat of hydride formation more negative than −6.5 kcal mole^{-1} H can have an electrochemical capacity of 340–430 mA h g^{-1}. However, if a Ti/Zr-based alloy has a calculated heat of hydride formation between −6.0 and −4.5 kcal mole^{-1} H, it will only have a capacity of 230−310 mA h g^{-1}, the same range as that of rare earth-based alloys. In this case, the rate capability and working potential of the Ti/Zr alloy is higher and similar to that of a rare earth-based alloy. Figs. 1 and 2 give the half-cell discharge curves of a Ti/Zr-based and rare earth-based alloys, respectively. The Ti/Zr-based alloy has 347 mA h g^{-1} at 100 mA g^{-1} current (385 mA h g^{-1} at 50 mA g^{-1} current, not shown), while the rare earth metal-based alloy gives less than 300 mA h g^{-1}.

Table 2
The comparison of the electrochemical performance of AB_x Ti/Zr-based and AB_x rare earth-based alloys

Performance	Ti/Zr alloy	Rare earth-based alloy
Capacity (mA h g^{-1})	250–430	230–310
Electrode preparation	Dry pressing	Dry or wet pasting
Activation before assembly	Required	Not needed
Rate capability	Good/excellent	Excellent
Cycle life	Good/excellent	Good/excellent

Table 1
Some useful hydrogen storage electrode alloys

Alloy no.	Composition	C (mA h g^{-1})	H_h (kcal mole^{-1} H)
601	$Ti_{10}Zr_{20}Ni_{35}Cr_{3.5}Mn_{4.5}V_{25}Al_{2.0}$	375	−7.10
602	$Ti_{24}Zr_{17}Ni_{41}Cr_{2.0}Mn_{7.0}V_{9.0}Al_{0.0}$	358	−6.90
603	$Ti_{22}Zr_{18}Ni_{40}Cr_{4.0}Mn_{8.0}V_{7.0}Al_{1.0}$	335	−6.65
604	$Ti_{8}Zr_{29}Ni_{44}Cr_{3.0}Mn_{10.0}V_{3.0}Mm_{2.0}$	360	−7.01
605	$Ti_{9}Zr_{29}Ni_{47}Cr_{2.0}Mn_{10}Nb_{2.0}Mm_{2.0}$	322	−6.86
606	$Ti_{30}Zr_{10}Ni_{47}Cr_{2.0}Mn_{7.0}Nb_{3.0}$	308	−5.94
607	$Ti_{10}Zr_{30}Ni_{48}Cr_{1.7}Mn_{7.0}Nb_{3.0}Hf_{0.3}$	334	−6.80
608	$Ti_{12}Zr_{27}Ni_{48}Cr_{1.5}Mn_{8.0}V_{1.5}Mm_{2.0}$	354	−6.90
609	$Ti_{10}Zr_{29}Ni_{47}Cr_{2.0}Mn_{8.0}V_{4.0}Al_{1.0}$	342	−6.70
610	$Mm_{16}Ni_{58}Co_{10}Mn_{9.4}Al_{5.0}Ti_{1.0}$	295	−4.81
611	$Mm_{17}Ni_{61.6}Co_{12.5}Mn_{6.7}Al_{2.2}$	285	−4.71
612	$Mm_{16.8}Ni_{59.5}Co_{12.4}Mn_{6.7}Al_{4.5}$	280	−4.72
613	$Mm_{16}Ni_{64.9}Co_{10.4}Mn_{4.8}Al_{4.0}$	295	−4.44
614	$Mm_{16.4}Ni_{60}Co_{14}Mn_{4.9}Al_{4.7}$	275	−4.52
615	$Mm_{16}Ni_{74}Sn_{5.0}Mn_{4.0}Mo_{1.0}$	285	−4.53

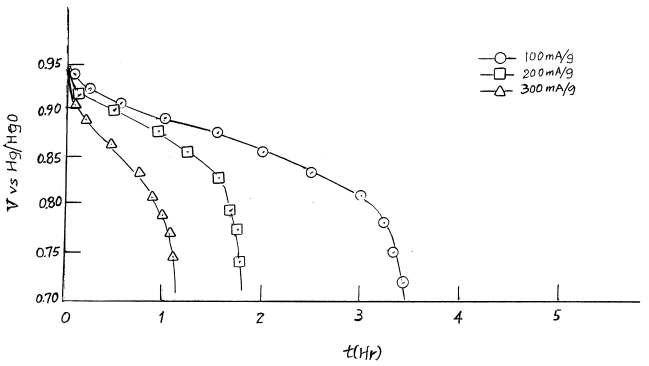

Fig. 1. The half-cell discharge curves of $Ti_{9.0}Zr_{22.0}Ni_{34.5}Cr_{3.0}Mn_{8.2}V_{23.0}Si_{0.3}$.

4. The state of commercial nickel hydride batteries

4.1. The manufacture process [30–33]

The making of nickel hydride batteries mainly includes: (1) negative hydride electrode line, (2) nickel positive electrode line, (3) cell assembly line, and (4) cell formation line. The active material in the negative electrode is the hydrogen storage alloy(s). The negative electrode can be made by a pasting method or a dry pressing process with or without sintering. The current collector substrate is nickel or nickel plated steel or copper in the form of mesh, perforated foil or expanded sheet. The pasting method requires slurry preparation but generally gives a better uniformity of the thickness, while the dry pressing plus sintering method will give a better rate performance. Furthermore, the pasting method, in general, is not suitable for a Ti/Zr-based alloy which requires pre-activation such as alkaline solution treatment before cell assembly. The nickel positive electrode generally is made by a pasting method in which the slurry of active material $Ni(OH)_2$ with additives is impregnated into the nickel foam substrate. The additives include fine powders of Co, CoO, $Co(OH)_2$, Zn, ZnO and other metal oxides. In the cell assembly process, cells can be made in a cylindrical or prismatic type. In a sealed type cell, the N/P ratio, i.e. the capacity ratio between the hydride negative electrode and the nickel positive electrode, is very critical to the internal pressure and the safety. During over-charge, a higher N/P cell will give a better oxygen recombination and therefore a lower steady internal pressure. However, the working potential is lower, and the cost is more for a N/P ratio higher than 2.0. A typical N/P ratio is between 1.20 and 1.70. After cell assembly, cells made are not ready to be used and have to be activated. The activation method [32,33] includes the thermal-activation and electrochemical activation. To reduce the time in the electrochemical activation, a thermal activation is often applied first at a temperature between 40 and 65°C. The thermal-activation will speed up the uniform electrolyte distribution across the electrodes and the surface cleaning in the negative hydride electrode. An electrochemical activation is done by charge/discharge cycles in a low current rate, typically below 0.5 c rate, preferably 0.1–0.2 c-rate. 1 c-rate is the current that a cell discharges to the cut-off voltage (1.0 V) in 1 h. The current of a 0.2 c-rate is one fifth of 1 c-rate current. The low rate current charge/discharge activation will assure the uniform current distribution leading to the uniform volume expansion/contraction in the early stage, the increasing of fresh surface and the reducing of premature gas generation before fully charge. It also gives a better charging efficiency. After activation, the cells are ready for use.

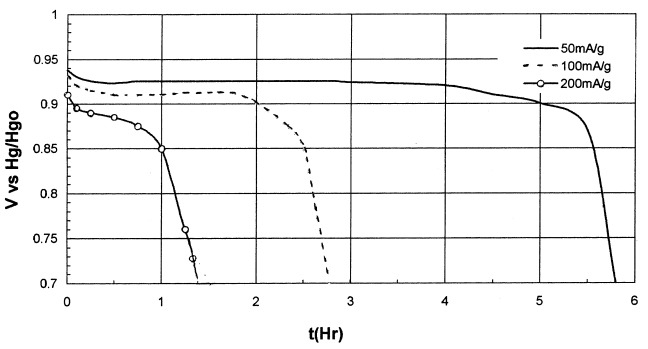

Fig. 2. The half-cell discharge curves of $Mm_{16.0}Ni_{74.0}Sn_{5.0}Mn_{4.0}Mo_{1.0}$ alloy.

4.2. Performance

The performance of a nickel hydride cell depends on many factors including the electrode preparation, active material and its amount, the additives in each electrode, N/P ratio, volume and the concentration of KOH electrolyte, separator and activation. In general, a well-made NiMH cell can show very good electrochemical properties. The electrochemical performance of a NiMH cell includes:

4.2.1. High capacity

The capacity of a NiMH cell keeps increasing from time to time. For example, the capacity of a AAA cell increases from 500 in 1996 to 550, then 600 and now up to 700 mA h. The energy density is up to 75–85 w h kg^{-1}. Fig. 3 gives discharge curves of a typical 650 mA h AAA cell we made using a Ti/Zr-based alloy.

4.2.2. High average working potential

The capacity ratio above 1.20 V to the total is an indicator to compare the working potential of different cells. Fig. 4 shows the discharge curves of a AAA-size cell using a mischmetal-based alloy at 0.2, 0.5 and 1 c-rate

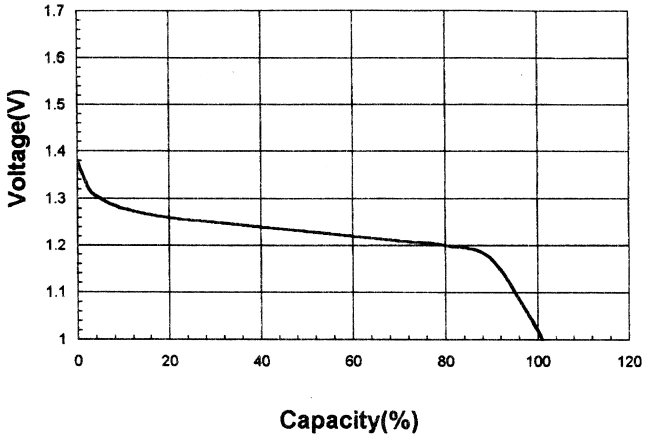

Fig. 3. A typical discharge curve at 1 c-rate for AA-650 mA h cell using a Ti/Zr-based alloy $Ti_{10.0}Zr_{30.0}Ni_{48.0}Cr_{2.0}Nb_{3.0}Mn_{7.0}$.

currents. It indicates that the capacity ratio above 1.20 V to the total is about 80% at 1 c-rate.

4.2.3. Excellent rate capability

The capacities at 1, 0.5 and 0.2 c-rate are very close, the difference is less than 4% (Fig. 4). For a high rate NiMH Sc size cell, it can discharge up to 20 c-rate (50 A current), the power is higher than 500 w kg^{-1} at fully charge and 350 w kg^{-1} at almost fully discharge, equal to or better than a NiCd Sc-size cell. But a NiMH cell delivers about twice the current because of double capacity for the same c-rate. Fig. 5 shows the discharge curves of a high rate NiMH Sc-size cell.

4.2.4. Low self discharge rate

The charge retention after 1 month storage at ambient temperature is above 80%.

4.2.5. Long cycle life

A typical charge/discharge cycle life of a NiMH cell is higher than 500 cycles at 1 c-rate charge–discharge cycle, 100% deep of discharge. It is noted that at the end of the life, the capacity of the cell still has about 80% of the initial capacity.

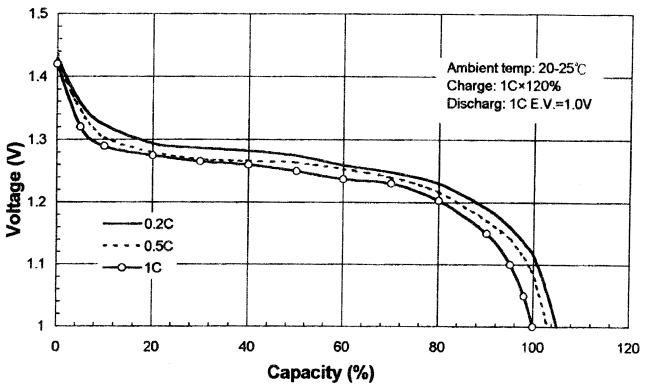

Fig. 4. The discharge curves of a AAA cell using a mischmetal-based alloy at 0.2, 0.5 and 1.0 c-rates.

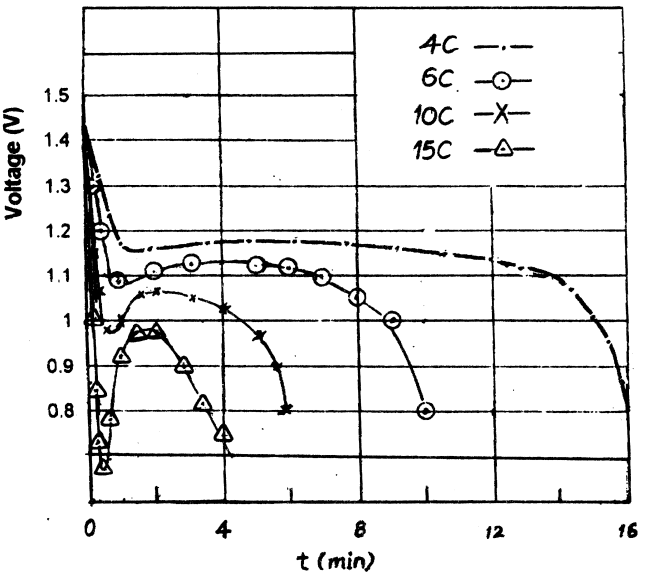

Fig. 5. The discharge curves of a typical NiMH Sc-size (1 c-rate = 2.50 A).

4.3. Applications

The mass commercialization of NiMH cells began in the early 1990s and was in the communication cellular phone market initially. The applications of NiMH cells since have broadened to many areas: (1) cellular phones, (2) cordless phones, (3) toys, (4) portable computers, (4) CDs, (5) camcorders, (6) power tools, (7) cordless and two-way radios, (8) UPS (uninterrupted power source), (9) EV, especially electric bikes. It is expected that NiMH batteries will increase the applications along with the new portable/wireless electronic products and that NiMH batteries will penetrate to stand-by power sources as well as energy storage systems in the near future.

5. Conclusion

Some of the hydrogen storage alloys can reversibly store hydrogen to form hydride and release hydrogen electrochemically. A semi-empirical electrochemical and thermodynamic method can be used to develop/screen the hydrogen storage alloys for rechargeable hydride electrode application. This method is suitable both for Ti/Zr-based and rare earth metal-based alloys. The Ti/Zr-based alloys have a higher capacity up to 430 mA h and the capacity of rare earth metal-based alloys is no higher than 320 mA h g^{-1}, following the restriction of heat of hydride formation. However, a higher capacity often associates with a lower rate capability and working potential.

The combination of a hydride electrode and a nickel

positive electrode to form a nickel hydride battery has been very successful. The performance of a NiMH cell is excellent, superior than a NiCd cell. There are many applications for NiMH batteries. NiMH cells are on the way to replace the market of NiCd cells.

References

[1] O.J. Kleppa, J. Chem. Phys. 80 (1978) 3452.
[2] G. Boureau, O.J. Kleppa, J. Chem. Phys. 65 (1976) 3915.
[3] O.J. Kleppa, M.E. Melnichk, T.V. Charlu, J. Chem. Thermodyn. 5 (1973) 595.
[4] R.H. Wiswall, J.J. Reilly, Metal hydrides for energy storage, Proc. 7th Intersociety Energy Conversion Eng. Conf., San Diego, 1972, p. 1342.
[5] R. Wiswall, Hydrogen Storage in Metals, Hydrogen in Metals II, 1978, pp. 201–242.
[6] K. Hong, ECD Quarterly reports, 1981–1985.
[7] K. Sapru, K. Hong, M. Fetchenko, S. Venketasan, US Pat. No. 4,51,400 (1985).
[8] E.W. Justi et al., Energy Conversion 10 (1970) 183–187.
[9] K.D. Beccu, US Pat. No. 3,669,745 (1972) and 3,824,131 (1974).
[10] M.A. Gujalar, H. Buchner, K.D. Beccu, H. Saufferer, Proc. 8th Int. Power Sources Conf., 1973, pp. 79–91.
[11] G. Bronoel, J. Sarradin, M. Bonnemay, A. Percheron, J.C. Achaed, L. Schlapbach, Int. J. Hydrogen Energy 1 (1976) 251–254.
[12] A. Percheron-Guegan, J.C. Achaed, J. Sarradin, G. Bronoel, Proc. Int. Conf. in Hydrides for Energy Storage, 1979, p. 485.
[13] J. Dunlop, M.W. Earl, G. van Ommering, US Pat. No. 3,959,018 (1976).
[14] F.G. Will, US Pat. No. 3,874,928 (1975).
[15] J. Dunlop, J. Stockel, US Pat. No. 4,112,199 (1978).
[16] J.G. Willems, Philips J. Res. 39 (1984) 1.
[17] J. Willems, J. van Beek, J. Buschow, J. Kurt, US Pat. 4,487,817 (1984).
[18] K. Hong, US Pat. No. 4,849,205 (1989).
[19] K. Hong, US Pat. No. 5,006,328 (1991).
[20] T. Gamo, Y. Moriwaki, T. Iwaki, US Pat. No. 4,946,446 (1990).
[21] K. Hong, Taiwan Pat. No. 36351 (1990).
[22] K. Hong, H. Hong, K. Kong, US Pat. No. 5,552,246 (1996).
[23] K. Hong, US Pat. No. 5,773,680 (1998).
[24] K. Hong, US Pat. No. 5,536,591 (1996).
[25] K. Hong, US Pat. No. 5,501,917 (1996).
[26] K. Hong, US Pat. No. 5,766,799 (1998).
[27] C.C. Chuang, Master Thesis, Tsing Hua University, Taiwan, 1993.
[28] Y.L. Po, Master Thesis, Tsing Hua University, Taiwan, 1993.
[29] T.C. Hsieh, Master Thesis, Tsing Hua University, Taiwan, 1993.
[30] K. Hong, H. Hong, K. Hong, US Pat. No. 5,541,017 (1996).
[31] K. Hong, H. Hong, K. Hong, US Pat. No. 5,556,719 (1996).
[32] K. Hong, Abstract, ECS Meeting, Seattle, 1999.
[33] K. Hong, H. Hong, K. Kong, US Pat. No. 5,695,530 (1997).